Bollettino di Geofisica Teorica ed Applicata Vol. 56, n. 4, pp. 489-504; December 2015
DOI 10.4430/bgta0165

Surface seismic monitoring of a natural gas storage reservoir in the Po Plain (northern Italy)

G. Franceschina, P. Augliera, S. Lovati and M. Massa

Istituto Nazionale di Geofisica e Vulcanologia, Milano, Italy

(Received: January 31, 2014; accepted: November 28, 2015)

ABSTRACT In the framework of the pilot project for CO_2 geo-sequestration in the depleted gas storage field of Cortemaggiore (Po Plain, northern Italy), started by the Italian company STOGIT in 2004, a surface seismic monitoring has been planned. The monitoring aims to detect possible changes, especially in microseismicity of the area, caused by the injection activity designed to achieve CO_2 geo-sequestration at 1000-1500 m of depth. The monitoring focuses on the ground motion produced by small-magnitude, shallow-depth seismic events. The Milano department of the "Istituto Nazionale di Geofisica e Vulcanologia" is taking part in the project through the installation of a seismic network, consisting of three surface and four 100-m deep borehole sensors, located at distances ranging from 0.5 to 3.5 km from the planned injection point. In this work, we analyze the data recorded from May 2010 to April 2012, in order to determine the noise levels of the area and the detection capabilities of the network.

Key words: CO_2 geo-sequestration, seismic monitoring, seismic ambient noise, earthquake detection.

1. Introduction

Carbon dioxide Capture and Storage (CCS), the process by which carbon dioxide emissions from power plants and other industrial facilities are captured and stored underground, has been recognized by the Intergovernmental Panel on Climate Change (IPCC) as a promising option to tackle the global issue of climate change (Metz *et al*., 2005). In 2009, the International Energy Agency (IEA) published the first CCS Roadmap (IEA, 2009) and highlighted the need to undertake prompt actions to accelerate the development of CCS technologies. Indeed, as an example, in 2012, CO_2 emissions in the atmosphere reached the level of 31.6 Gt, increasing by 1.4% from 2011 and confirming a previously recognized trend (IEA, 2013a). According to the 2013 edition of the IEA Technology Roadmap for CCS, this technology is an integral part of any lowest-cost mitigation scenario where the increase of the long-term global average temperature is limited to less than 4°C (IEA, 2013b). In general, a CCS system consists of three stages: capture and separation of CO_2 emitted from large-scale fixed sources, transport to a storage site, and long-term isolation from the atmosphere. The last phase involves the permanent storage (sequestration) into suitable geological formations: deep saline aquifers, hydrocarbon fields, or coal fields. The review of worldwide storage capacities and carbon dioxide emissions

due to stationary sources, performed by IPCC in 2005, shows a good correlation between major emission sources and prospective sedimentary basins (Metz *et al.*, 2005). The potential for geological storage is generally evaluated based on the availability of suitable storage reservoirs—hydrocarbon reservoirs or deep saline formations located at depths of more than 800 m, where temperatures and pressures keep the CO_2 in a liquid or supercritical state. Under these conditions, a volume reduction greater than 97% is obtained for the stored gas. It is worth noting that CCS technology has been used at a large scale for decades, and currently there are 12 operational large-scale CCS projects throughout the world, which have the global capacity to prevent 25 Mt/year of CO_2 from reaching the atmosphere (Global CCS Institute, 2013). Some arguments have been expressed against CCS technologies, claiming that large-scale CCS will be an extremely expensive and risky strategy for achieving significant reductions in greenhouse gas emissions (Zoback and Gorelik, 2012). However, the above-mentioned projects have improved our understanding of processes within the reservoir and increased confidence in techniques to predict and monitor the long-term behavior of the injected CO_2.

The European capacity for geological storage of carbon dioxide was assessed by the project EU GeoCapacity within FP6, the 6th Framework Program of the European Community for research, technological development, and demonstration activity (EU Geocapacity, 2009a, 2009b). The conservative estimate provided by the project gives a total storage capacity of 117 Gt, with 96 Gt in deep saline aquifers, 20 Gt in depleted hydrocarbon fields, and 1 Gt in coal beds that cannot be mined. Considering that CO_2 emissions from large-point sources emitting more than 0.1 Mt/year amount to a total of 1.9 Gt/year, the estimated storage capacity corresponds to 62 years of geological storage. Deep saline aquifers also represent the main storage reservoirs in Italian territory. For Italy, the estimated storage capacities are 4.7 Gt, 1.8 Gt, and 0.07 Gt for deep saline aquifers, depleted hydrocarbon fields, and coal beds, respectively. Annual CO_2 emissions from the Italian large-point sources amount to 140 Mt/year.

Aiming to prove the feasibility of CCS projects at a national scale, ENEL, the largest Italian power company, is committed to build a CCS demonstration facility at Porto Tolle (north-eastern Italy). The facility aims to capture the CO_2 present in the flue stream from a power plant and then compress, transport, and store it in a deep saline aquifer. The project, funded by the European Union as part of the European Energy Program for Recovery (EEPR), involves retrofitting a 660 MW coal-fired power-generation facility with a post-combustion CO_2 capture system at the Porto Tolle plant (http://www.zeportotolle.com). In the meantime, in the frame of a collaboration agreement between ENEL and ENI, the major Italian integrated energy company, a CCS pilot project was initiated by constructing and operating a pilot CO_2 capture plant in Brindisi (southern Italy) and starting a project for geological storage of carbon dioxide in the natural gas reservoir of Cortemaggiore (northern Italy), the "CO_2 Cortemaggiore project". This latter activity was commissioned to STOGIT (SNAM group), Italy's leading operator in the storage of natural gas, in order to exploit the vast experience gained in this field by the company (http://www.stogit.it). The "CO_2 Cortemaggiore project" aims to verify the injection technique and involves activities that are similar to those of natural gas storage, which began in the field of Cortemaggiore in 1964. The quantity of CO_2 that will be injected into the reservoir will amount to 8 Mt/year for a maximum of three years. The project involves the construction of a well for the CO_2 injection in a sand layer already used for the storage of natural gas and located at 1.4 km

depth, and the construction of an above-ground plant for the CO_2 storage and injection. Also included is a control system that will provide both geochemical and seismic monitoring. In order to perform the surface seismic monitoring of the storage reservoir, the Milano department of the Istituto Nazionale di Geofisica e Vulcanologia (INGV) was commissioned to deploy a dense seismic network in the storage area (Fig. 1). The network, consisting of three surface and four 100-m deep borehole sensors, installed at distances ranging from 0.5 to 3.5 km from the planned injection point, operated from May 2010 to April 2012 in a continuous mode, collecting more than 280 Gb of data (Augliera *et al.*, 2011b, 2012). This work shows a preliminary analysis of the data recorded by the network during these two years of activity. In this period, CO_2 storage was not in operation. Velocity records are employed to establish both noise levels of the area and detection capabilities, and to investigate the different types of signals recorded during the pre-injection period.

2. Network design

The Po Plain (northern Italy), a very large (45,000 km^2) alluvial basin delimited by the Alps and Apenninic chains to the north and to the south, respectively, is characterized throughout by the presence of deep sediments with soft top layers. Indeed, the thickness of the Plio-Pleistocene sedimentary succession, which extents for the whole area, can reach 7000-8000 m at depocentres (Bigi *et al.*, 1992). The region is affected by a general compressive regime, with thrust systems in the central-eastern Southern Alps and buried active thrusts in the northern Apennines (Galadini *et al.*, 2005; Carminati *et al.*, 2010). Historical and current seismicity is observed both in correspondence to the Pedeapenninic Thrust Front, which borders the whole Po Plain to the south and in the central-eastern Southern Alps, with maximum magnitudes that decrease from east to west (http://emidius.mi.ingv.it/CPTI11/; http://csi.rm.ingv.it; http://bollettinosismico.rm.ingv.it; http://iside.rm.ingv.it). In particular, the recent May-June 2012 earthquake sequence was attributed to the reactivation of the Ferrara Arc, the easternmost buried thrust lying ahead of the Pedeapenninic Front (Fig. 1). The area to be monitored is located in the central part of the Po Plain, between the Pedeapenninic Thrust Front and the Pavia Arc, above a depleted natural gas reservoir, exploited by STOGIT since 1964 (Fig. 1). In this region, the Plio-Pleistocene sedimentary succession reaches a maximum depth of 2000-3000 m (Fantoni and Franciosi, 2010) and the reservoir is situated at a depth of between 1200 and 1500 m, in correspondence to a structural high where the presence of caprocks, consisting of 300 m of clay, ensures the seal of the deposit (http://www.stogit.it; Boiardi, 2012). The area is also characterized by high anthropogenic noise, due to the presence of important transportation routes and diffuse agricultural and industrial activities.

The geological storage of CO_2 should be monitored by seismic networks able to perform accurate locations of the micro-events induced by injection activities into the depths of the reservoir. Surface networks (Verdon *et al.*, 2010) cannot achieve this but, in favourable conditions of ambient noise, they can adequately locate small events (M_L 0.5) up to depths of about 2 km (Ugalde *et al.*, 2013). In order to plan the monitoring experiment, we performed preliminary analyses of ambient noise by applying the standard methodology introduced by McNamara and Buland (2004) to compute Probability Density Functions (PDFs) of the noise

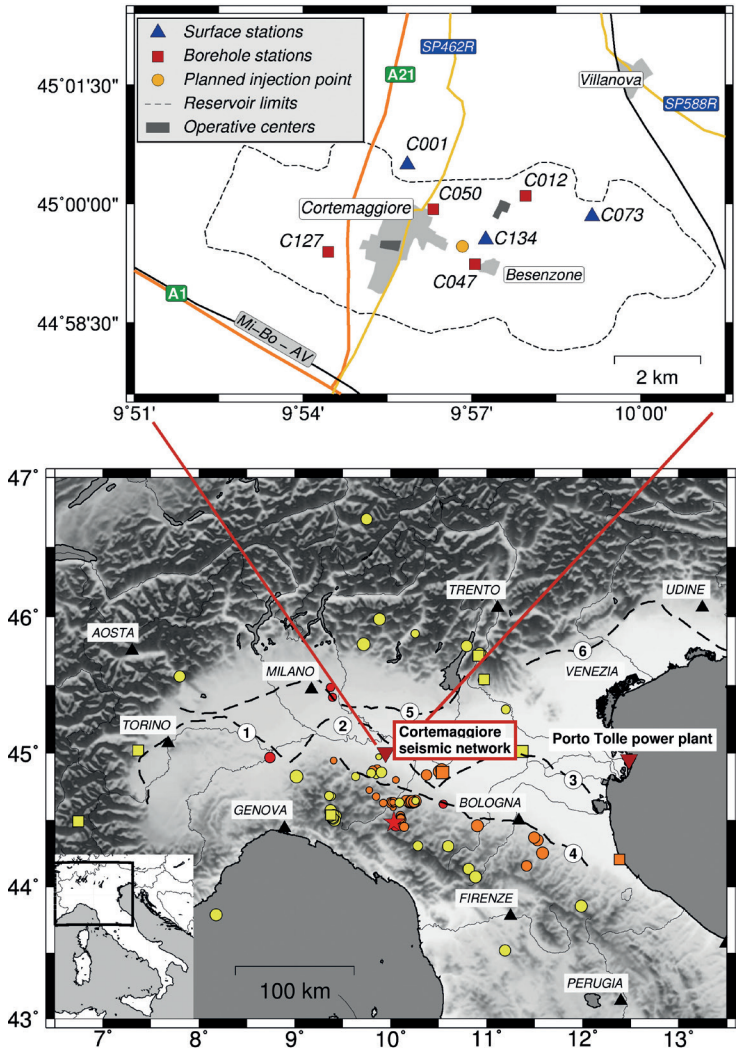

Fig. 1 - Upper map: Cortemaggiore seismic network with location of surface and borehole instruments (blue and red symbols, respectively). The planned injection point, the surface projection of the reservoir, and the main transportation routes (A1 and A21 highways and Milano-Bologna high-speed railway) are also indicated. Lower map: location of the Cortemaggiore seismic network and of the Porto Tolle power plant in the Po Plain area, and epicentres of the earthquakes recorded by the network during the period May 2010 - April 2012. Yellow, orange, and red symbols correspond to shallow (depth ≤ 18 km), intermediate (18 km < depth ≤ 35 km) and deep (depth > 35 km) events, respectively. Circles, squares, and stars indicate $M_L < 4.0$, $4.0 \le M_L < 5.0$, and $M_L \ge 5.0$ events, respectively. Dashed lines indicate the main tectonic features of the area. 1: Monferrato Arc; 2: Pavia Arc; 3: Ferrara Arc; 4: Pedeapenninic Thrust Front; 5: central Southern Alps boundary; 6: eastern Southern Alps boundary.

velocity power spectrum. One-hour ambient noise continuous recordings, obtained in the period that preceded the installation of the network, were reviewed. Recorded traces were baseline-corrected by removing a linear trend and deconvolved with the instrumental response. A 10% cosine shaped taper was applied before computing the FFT and, in order to reduce the variance, spectral amplitudes were smoothed with a Konno and Omachi (1998) window, with *b* parameter equal to 20. Fig. 2 shows the PDF of noise for one horizontal component recorded at the surface, compared with the reference Low – and High-Noise Models (LNM and HNM) of Peterson (1993). As expected, the area is generally characterized by elevated levels of noise. At

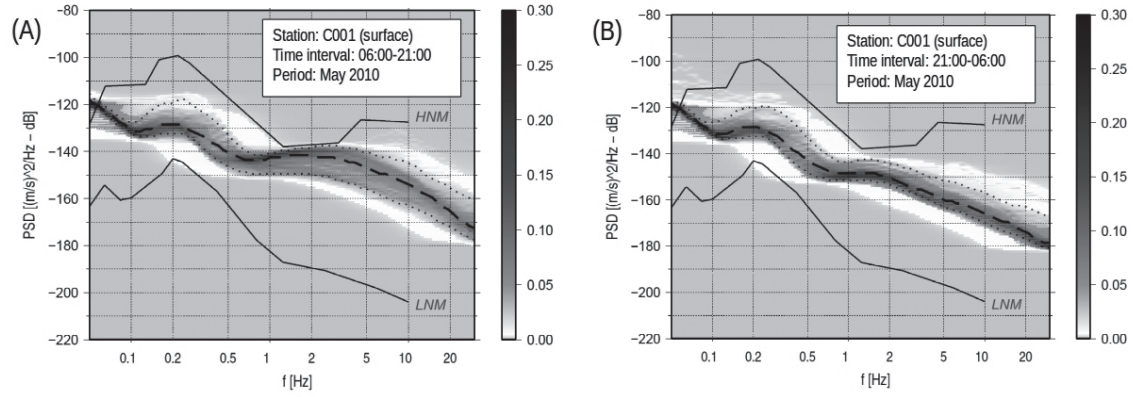

Fig. 2 - Daily (A) and nightly (B) levels of seismic ambient noise recorded at surface in the Cortemaggiore area during one month of monitoring. PDF of velocity power spectra are compared with the LNM and HNM, of Peterson (1993). The dashed line indicates the median of the power spectra distribution. Dotted lines indicate the 5th and 95th percentile. Station type and code, together with timing and monitoring period, are indicated in each panel.

night, the recorded average velocity power spectral density values, in units of dB with respect to 1 $(m/s)^2$/Hz, range from -150 to -170 dB in the frequency band 1-10 Hz. Diurnal recordings are characterized by noise levels that are 10 dB higher with respect to the records obtained at night.

Ambient noise measurements were employed to establish the detection threshold of the network to be installed in the area. A point source simulation of earthquakes characterized by different values of magnitude and distance was performed, in order to compare the power spectrum of the simulated earthquake with the observed power spectrum of ambient noise. A similar approach was adopted by Stabile *et al*. (2013) and by Tramelli *et al*. (2013). The velocity amplitude Fourier spectrum of S-waves, $V(f)$, recorded at hypocentral distance R, was modelled according to Brune (1970). The seismic wave attenuation was introduced by considering a R^{-1} dependence of geometrical spreading, a frequency dependence of the quality factor and a constant value of the k parameter of Anderson and Hough (1984). The model:

$$V(f) = \frac{C \cdot M_O}{R} \frac{2\pi \cdot f}{1 + \left(\frac{f}{f_C}\right)^2} \cdot \exp\left(-\frac{\pi \cdot R \cdot f}{\beta \cdot Q(f)}\right) \cdot \exp(-k\pi f) \qquad (1)$$

was assumed, where M_0 and f_c represent the seismic moment and the corner frequency of the simulated earthquake, respectively. $Q(f)$ is the frequency-dependent quality factor and β is the S-wave velocity. The constant C is given by: $C = F_S R_{\theta\phi} / 4 \pi \varrho \beta^3$ where F_S, $R_{\theta\phi}$, and ϱ are the free surface factor, the radiation pattern factor, and the density of the medium. We adopted β = 2.6 km/s; ϱ = 2.4 g/cm^3; F_S = 2 and $R_{\theta\phi}$= 0.63 for the RMS radiation pattern of S-waves (see Molinari *et al*., 2015). Attenuation studies of the area suggest $Q(f) = 82 f^{1.2}$ (Castro *et al*., 2013), and from comparisons between simulated and recorded events that occurred within a few tens of kilometres, we inferred an average value for k of 0.06 s (Augliera *et al*., 2010). Finally, for any M_0 value, the corner frequency of the event was computed assuming a constant stress drop scaling with $\Delta\sigma$ = 5 MPa (Lay and Wallace, 1995). For any fixed value of moment magnitude,

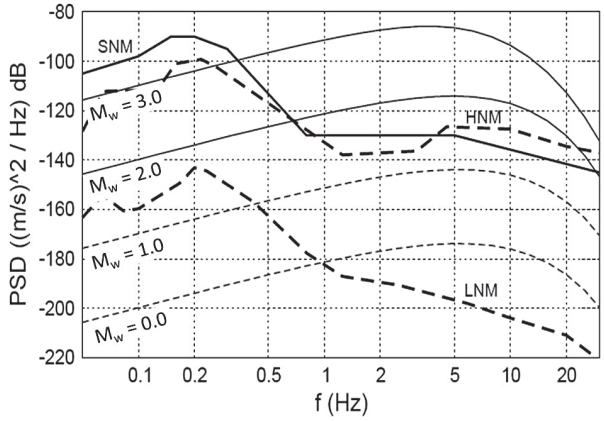

Fig. 3 - Simulated velocity power spectra for earthquakes occurring at 2-km hypocentral distance from the network. Power spectral densities of M_W = 0.0; M_W = 1.0; M_W = 2.0; and M_W = 3.0 events are compared with the maximum surface noise level of the area, inferred from the Seismic ambient Noise Measures (SNM), and with LNM and HNM of Peterson (1993). Solid and dashed lines indicate detectable and undetectable power spectra, respectively. Simulated power spectra are obtained by adopting Eq. 1 with k = 0.06 s (see text).

M_W, and hypocentral distance, R, we applied Eq. 1 to calculate $V(f)$ and a corresponding velocity power spectrum. The Power Spectral Density (PSD) was computed by assuming a constant duration of 5 s and the seismic moment was computed using the standard definition of M_W (Hanks and Kanamori, 1979). We defined the detection thresholds using the event-to-noise ratios of PSD between the simulated-earthquake and the median observed ambient noise. We calculated the mean value of the PSD ratio in the frequency band 1-25 Hz and considered an event to be detectable when the mean event-to-noise ratio, expressed in decibels, was greater than 15 dB. Under these conditions, we obtained M_W detection thresholds equal to 1.5, 1.7, and 2.0 for sources located at 1-, 2-, and 5-km hypocentral distance, respectively. A previous study, based on preliminary estimates of the average noise levels, shows similar results (Augliera *et al.*, 2011a). Fig. 3 shows, as an example, the earthquake-simulated power spectra compared with noise levels for sources located at a distance of 2 km.

3. The Cortemaggiore seismic network

Aiming to improve detection capabilities, it was decided in the framework of the project to complete the surface network with some additional borehole stations installed at a 100-m depth. Fig. 1 shows the final network configuration with four borehole sensors installed at distances ranging between 0.5 and 3.0 km from the planned injection point and three surface stations located at comparable distances. Overall, the network extends over an area of (6.5 x 2.5) km^2. All stations are equipped with 24-bit digital recorders (Lennartz M24/NET) equipped with GPS time signal. Lennartz LE-3D/BH and Lennartz LE-3Dlite MkII sensors were used for borehole and surface installations, respectively. The borehole and surface sensors have similar characteristics with 136 dB dynamic range, 1-80 Hz band-pass frequency and 400 V/m/s sensitivity. Data-loggers have ±10 V full scale and are equipped with a 60 Gb HD where data can be archived in different formats (miniSEED, GSE, SEG-Y, ASCII). All stations are equipped with power supply and buffer battery, kept charged with solar panels. An Ethernet

connection with standard TCP/IP protocol allows operating the Ethernet interface necessary to perform data-logger setup, checkup operations, data plot, and data export. The FreeBSD operating system, running on the M24/NET, allows fast download of large quantities of data through standard FTP applications. Several acquisition configurations were tested during the early installation of the network. Based on the tests carried out from February to April 2010, we decided to record the data in M24/ASCII format daily files and to set the acquisition sampling rate to 100 Hz. From May 2010 to April 2012, the network operated almost continuously, recording about 280 Gb of data. Indeed, during the operational period, the days of malfunctioning were limited to less than 1%. The final data set, is composed of about 360,000 SAC binary format (Tapley and Tull, 1992) hourly files, derived from the post-processing of the M24/ASCII format files recorded by Lennartz data loggers, for a total of 500 Gb disk space.

4. Seismic ambient noise levels

Preliminary estimations of ambient noise, performed by root mean square measurements on continuous recording of noise, indicate a reduction of a factor of 2.6 moving from daily to nightly surface recordings, with average values of (9.8×10^{-7}) and (3.8×10^{-7}) m/s, respectively. The data recorded by all stations of the network during the pre-injection period were employed to confirm this observation and to extend the analysis to borehole data. The frequency content of the recorded ambient noise was investigated by means of the velocity power spectral density computation, adopting the standard approach of McNamara and Buland (2004) to handle the statistics. Power spectra are compared with the reference Low- and High-Noise Models (LNM and HNM) of Peterson (1993). Surface and borehole stations can be grouped in two distinct sets characterized by negligible differences among single stations. Hereinafter we thus present measures obtained at single surface and borehole installations as results representative of all surface and borehole installations, respectively. Fig. 4 shows the daily variability of ambient noise recorded at the surface and at 100 m of depth. As previously assessed, the nightly ambient noise in the frequency band 1-25 Hz is on average 10 dB lower than the noise recorded during the day for stations installed at the surface. For borehole stations, the daily variability is reduced to 5 dB. Unfortunately, due to the elevated anthropogenic noise that characterizes the area, records collected at 100 m of depth during the day, show, on average, the same level of noise of surface records obtained at night. However, the ambient noise recorded at that depth is characterized by lower variability. Anthropogenic activities are also evidenced by the monthly variability of noise. Fig. 5 shows an example of noise measurements performed in winter and in summer, when farming activities are more intense. In the latter period, the noise variability at surface stations can reach 25 dB in the frequency band 5-20 Hz. Instead, a 10 dB variability is observed at 100 m of depth.

5. Detection analysis

The procedure described above for establishing the detection capabilities of stations installed in this area was applied to the whole network with the aim of assessing the improvement

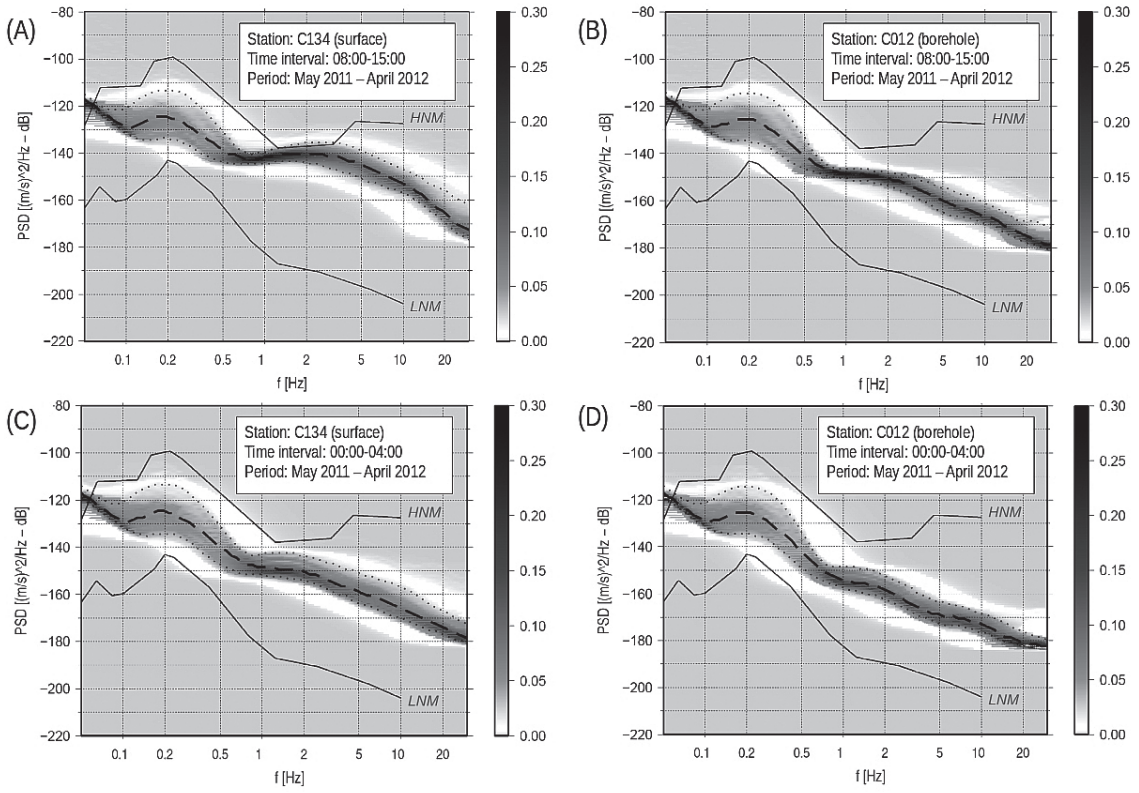

Fig. 4 - Surface [panels (A) and (C)] and borehole [panels (B) and (D)] levels of seismic ambient noise recorded in the Cortemaggiore area during one year of monitoring. PDF of velocity power spectra are compared with the LNM and HNM of Peterson (1993). The dashed line indicates the median of the power spectra distribution. Dotted lines indicate the 5th and 95th percentile. Station type and code, together with timing and monitoring period, are indicated in each panel.

obtained thanks to the installation of borehole sensors. We applied Eq. 1 to simulate earthquakes of different magnitudes occurring at different distances from the network by using the above reported values of β; ϱ; $R_{\theta\phi}$ and Q (f), and by setting F_S equal to 1 and 2 for borehole and surface stations, respectively. Stress drop and k values were inferred through comparison between simulated and observed S-wave amplitude Fourier spectra. Theoretical spectra were simulated for stress drop values of 1; 5 and 10 MPa and k values of 0.06; 0.07 and 0.08 s, for all the events with M_L>2.5 and R>50 km recorded by the network in the period May 2010 - April 2012. Simulated and observed amplitudes were compared by computing the Mean Residuals (MR), and the Mean Absolute Residuals (MAR) in the frequency band 1-25 Hz. For each frequency, the residuals were calculated as the difference between the logarithmic values of the observed and simulated spectral amplitudes. In order to choose the stress drop and k values for the computation of the network detection threshold, we calculated mean MR values and mean MAR values for all the events with M_L>2.5 and R>50 km recorded by the network. The best fit solution, corresponding to stress drop and k values of 1 MPa and k=0.07 s, respectively, allowed us to obtain mean MR values of 0.03 and -0.03 for borehole and surface stations, respectively, and mean MAR values of 0.26 and 0.27 for borehole and surface stations, respectively. In this case, 85% of the analyzed events show MAR<0.4. Fig. 6 shows some

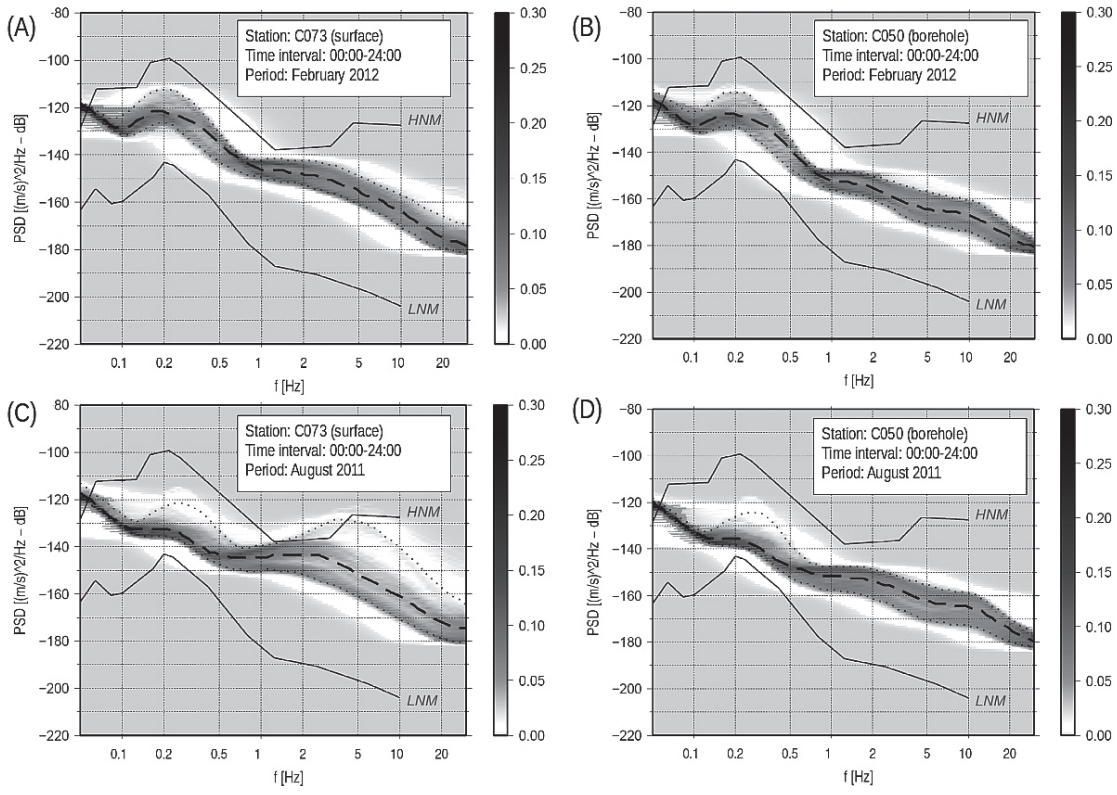

Fig. 5 - Seasonal variations of seismic ambient noise recorded at stations C073 [panels (A) and (C)] and C050 [panels (B) and (D)] during one month of monitoring. PDF of velocity power spectra are compared with the LNM and HNM of Peterson (1993). The dashed line indicates the median of the power spectra distribution. Dotted lines indicate the 5th and 95th percentile. Station type and code, together with timing and monitoring period, are indicated in each panel.

examples of fit between theoretical and observed spectral amplitudes. For application purposes, we decided to express the final outcome of the work as detection thresholds of local magnitude, M_L. According to Hanks and Boore (1984), the seismic moment was related to M_L using the bilinear relation:

$$\text{Log } M_0 = 1.5\, M_L + 9.0 \quad (M_L \geq 3.0) \qquad (2)$$
$$\text{Log } M_0 = 1.0\, M_L + 10.5 \quad (M_L < 3.0)$$

Examples of power spectra models obtained with different M_L values at borehole and surface stations for R = 2 km are shown in Fig. 7. In this figure, the simulated power spectra are compared with Peterson (1993) curves and with PDF distributions of noise recorded at 100 m of depth and at the surface. Surface and borehole detection thresholds were then established by computing the signal-to-noise ratio between simulated power spectra and median values of the observed noise distributions. For different values of R, PSD differences between the earthquake signal and the ambient noise, measured in the frequency band 1-25 Hz, are shown as a function of magnitude in Fig. 8. It is apparent from the figure that installations at a depth of 100 m imply an increase of the detection capability of about 0.3 units of magnitude. Indeed, borehole sensors are characterized by average noise levels 10-15 dB lower than surface sensors, but signals recorded in the well are on average two times weaker than the surface ones. According to the

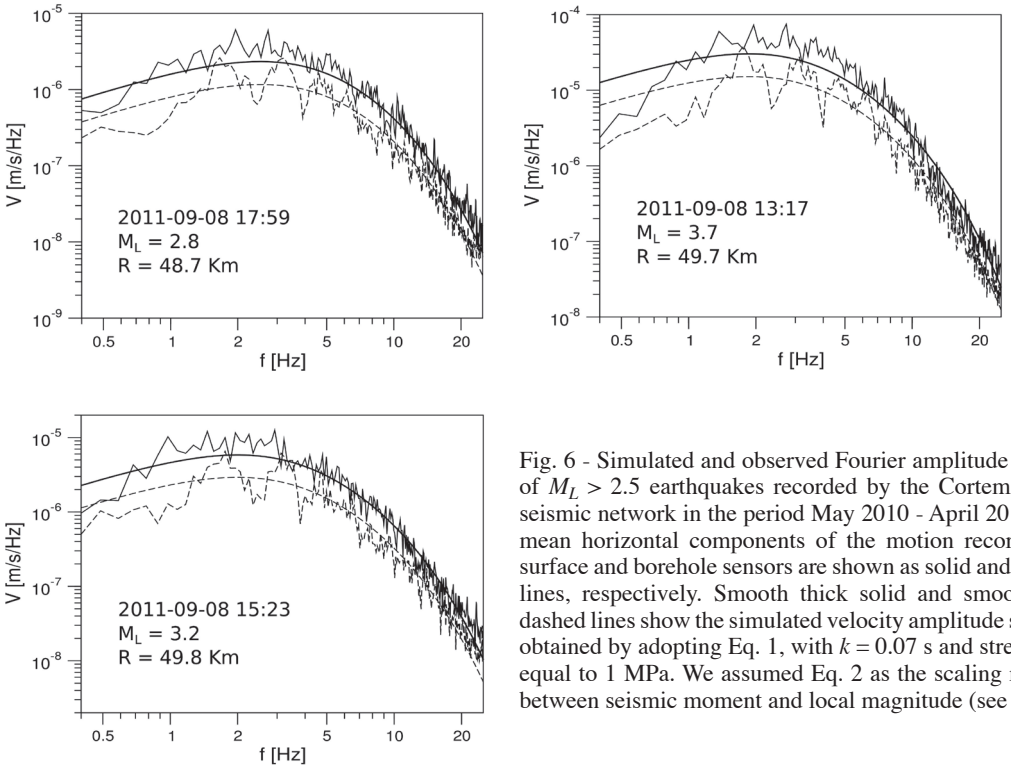

Fig. 6 - Simulated and observed Fourier amplitude spectra of $M_L > 2.5$ earthquakes recorded by the Cortemaggiore seismic network in the period May 2010 - April 2012. The mean horizontal components of the motion recorded by surface and borehole sensors are shown as solid and dashed lines, respectively. Smooth thick solid and smooth thin dashed lines show the simulated velocity amplitude spectra, obtained by adopting Eq. 1, with $k = 0.07$ s and stress drop equal to 1 MPa. We assumed Eq. 2 as the scaling relation between seismic moment and local magnitude (see text).

energy of the incident wave field, borehole recordings can show spectral peaks and holes due to the interference between up-and-down seismic waves. However, theoretical simulations performed by Eq. 1 show that, on average, an attenuation model defined in terms of the spectral decay parameter, k, can also adequately reproduce spectral amplitudes observed at depth. By adopting the above-described detection criterion, namely that the mean PSD event-to-noise ratio in the frequency band 1-25 Hz is greater than 15 dB in order to recognize a seismic event, we obtain the threshold magnitudes of Table 1. The listed values refer to both borehole and surface sensors. It is evident from Table 1 that the network is unable to detect micro-earthquakes ($M_L < 0.0$) possibly induced by carbon dioxide injection, because the storage reservoir is located between 1.2- and 1.5-km depth (Nicol *et al.*, 2011). Instead, small (M_L 0.5) earthquakes that might occur at the depths of the reservoir would be fully detectable, confirming that surface networks cannot be used to monitor the micro-fracturing process occurring at the injection point but are however capable to detect small shallow earthquakes not felt by the population.

6. Automatic signal detection

In this preliminary analysis, we decided to employ a standard STA/LTA algorithm in order to detect transient signals above the average noise level. Frequency content, duration, coincidence conditions between the recording stations, amplitude ratio between vertical and horizontal components of the ground motion, analyzed through visual inspection of the detected signals, were considered to distinguish between seismic events and transient signals of anthropogenic

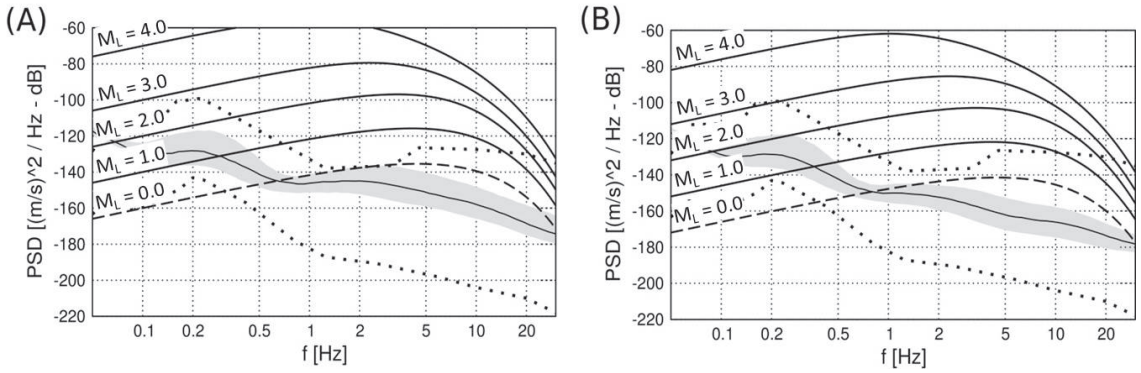

Fig. 7 - Simulated velocity power spectra for earthquakes occurring at 2 km hypocentral distance from the network. Power spectral densities of $M_L = 0.0$; $M_L = 1.0$; $M_L = 2.0$; $M_L = 3.0$; and $M_L = 4.0$ events are compared with the average surface (left panel) and borehole (right panel) noise levels of the area (gray area and thin solid line) and with LNM and HNM (dotted lines) of Peterson (1993). Thick solid and dashed lines indicate detectable and undetectable power spectra, respectively. Simulated power spectra are obtained by adopting Eq. 1, with $k = 0.07$ s and stress drop equal to 1 MPa. We assumed Eq. 2 as the scaling relation between seismic moment and local magnitude (see text).

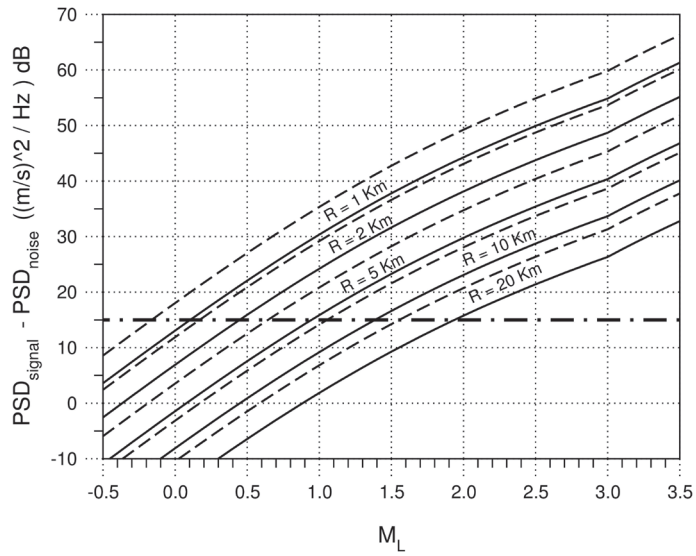

Fig. 8 - Surface (solid lines) and borehole (dashed lines) detection thresholds for earthquakes located at different hypocentral distances from the network. The signal-to-noise ratio, represented in terms of power spectral density difference, is measured in the frequency band 1-25 Hz. The dotted-dashed line shows the chosen detection level, corresponding to an amplitude ratio of 15 dB.

Table 1 - Detection thresholds of the Cortemaggiore seismic network.

Hypocentral distance (km)	Minimum detectable M_L (surface)	Minimum detectable M_L (100 m depth)
1	0.1	-0.2
2	0.5	0.2
5	0.9	0.6
10	1.4	1.1
20	1.9	1.6

origin. The recorded time sequences were filtered in different bands of frequency. In particular, we considered the frequency band 2-15 Hz, that, removing the low-frequency component, minimizes the number of detected teleseisms. We adopted long time and short time averages of 100 and 1 s, respectively, trigger and de-trigger threshold levels equal to 5 and 2, respectively, and a maximum duration of 2 s for the network trigger. The automatic procedure detects an event by requiring the coincidence of the trigger at three or more stations of the network. Table 2 summarizes the results obtained by applying the detection procedure to continuous data recorded in the period May 2010 - April 2012. Detected events were classified according to the following scheme:

A - seismic events located inside the network (hypocentral distances < 10 km);

B - seismic events located outside the network (hypocentral distances between 10 and 300 km);

C - regional events (hypocentral distances > 300 km) and teleseisms (hypocentral distances > 2000 km);

D - beats with characteristic frequencies of 3-4 Hz;

E - generic transient noise with variable frequency content.

Examples of automatically detected events are presented in Figs. 9 and 10.

26% of the signals detected by the automatic system are recognized as seismic events, 92.3% of which are due to seismic sources located less than 300 km from the network. Locations are taken from the Italian Seismic Bulletin (http://bollettinosismico.rm.ingv.it). In particular, 11 events out of the total 120 recorded earthquakes, are seismic events not included in the bulletin, characterized by S-P time intervals around 4-5 s, therefore classifiable as B-type events. Fig. 1 shows the epicentres of the earthquakes of type A and B recorded by the seismic network during the pre-injection period. Earthquakes with the smaller epicentral distances (between 10 and 70 km) are located in the Parma and Piacenza areas (Val di Taro and Valle del Trebbia) and are characterized by local magnitudes between 1.7 and 4.1. Regional events characterized by greater magnitudes and distances have also been recorded by the network. The strongest events recorded by the network during the monitoring period occurred in the Po Plain: the M_L 4.8 Ferrara-Rovigo event of July 17, 2011; the M_L 4.9 Parma event of January 25, 2012; and the M_L 5.4 event that occurred on January 27, 2012 in the Frignano area.

36.6% of the detected events can be classified as beats, with characteristic frequency around 3-4 Hz, maybe due to anthropogenic sources located near the network. The remaining 37.4%, classified as “generic noise”, are due to different types of anthropogenic sources. Indeed, as

Table 2 - Number of events recorded by the Cortemaggiore seismic network in the period: May 2010 - April 2012. The bracketed numbers refer to events not included in the Italian Seismic Bulletin.

type	Number and percentage of events detected in the period: May 2010 - April 2012	
A	1	0.2 %
B	119 (11)	23.8 %
C	10	2.0 %
D	183	36.6 %
E	187	37.4 %
total	500	100.0 %

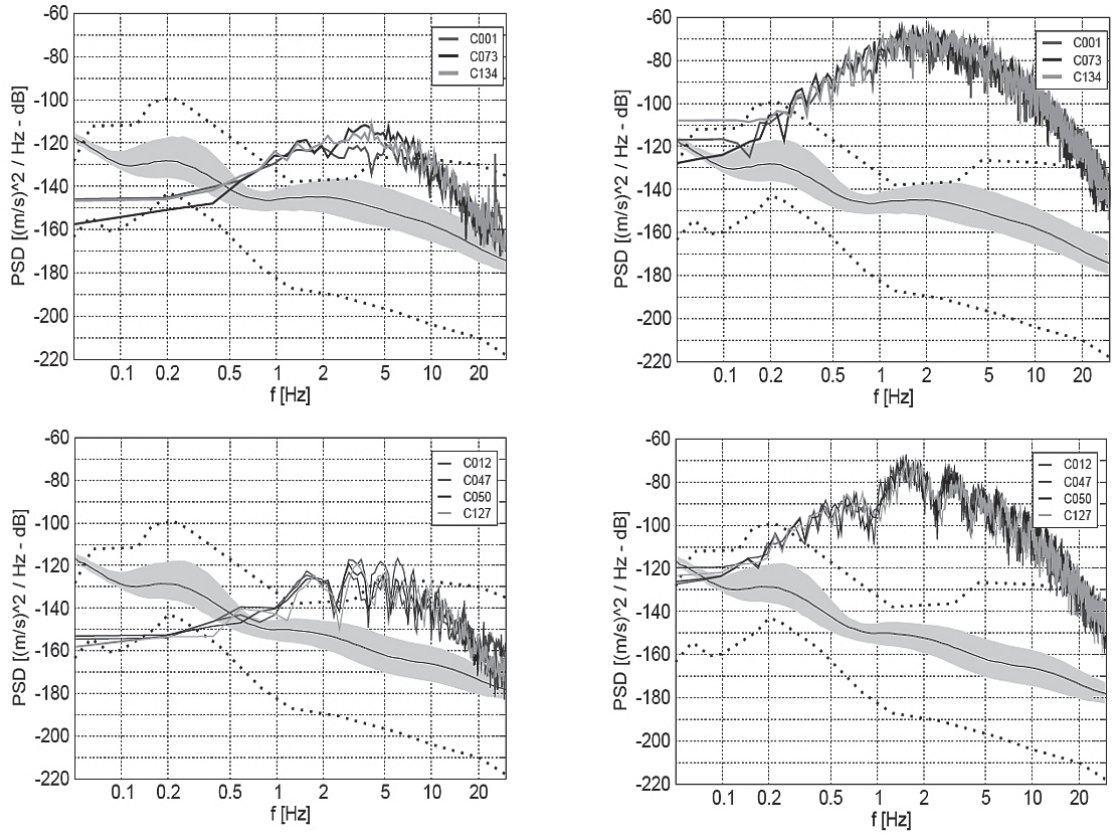

Fig. 9 - Left panels: horizontal component velocity power spectra of the M_L 1.7 earthquake occurred on August 1, 2011, at 9.1 km hypocentral distance from the network. Right panels: horizontal component velocity power spectra of the M_L 4.9 Parma earthquake occurred on January 25, 2012, at 60.0-km hypocentral distance. Upper and lower panels show the power spectra recorded with surface and borehole stations, respectively. Recorded power spectra are compared with the seismic ambient noise measurements (gray areas) and with the reference noise levels of Peterson (1993) (dotted lines).

previously mentioned, the area is characterized by particularly high levels of noise due to the presence of important transportation routes and both agricultural and industrial activities. Fig. 9 shows two examples of earthquakes automatically detected by the system. These records have been classified as A- and B-type events, associated with the M_L 1.7 earthquake that occurred on August 1, 2011, at 9.1 km hypocentral distance and to the M_L 4.9 Parma earthquake of January 25, 2012, (60 km hypocentral distance), respectively. Non-seismic signals detected by the system are shown in Fig. 10. Note the peculiar frequency content of the D-type event and the high variability of the power spectral levels recorded by different stations of the network for the E-type event.

7. Conclusions

The analysis of the data recorded from May 2010 to April 2012 by the surface seismic network, installed in the framework of the "CO_2 Cortemaggiore project", allows us to establish the detection capabilities of the surface seismic monitoring of the storage reservoir. In the frequency band 1-25 Hz, surface stations are characterized by an average level of velocity

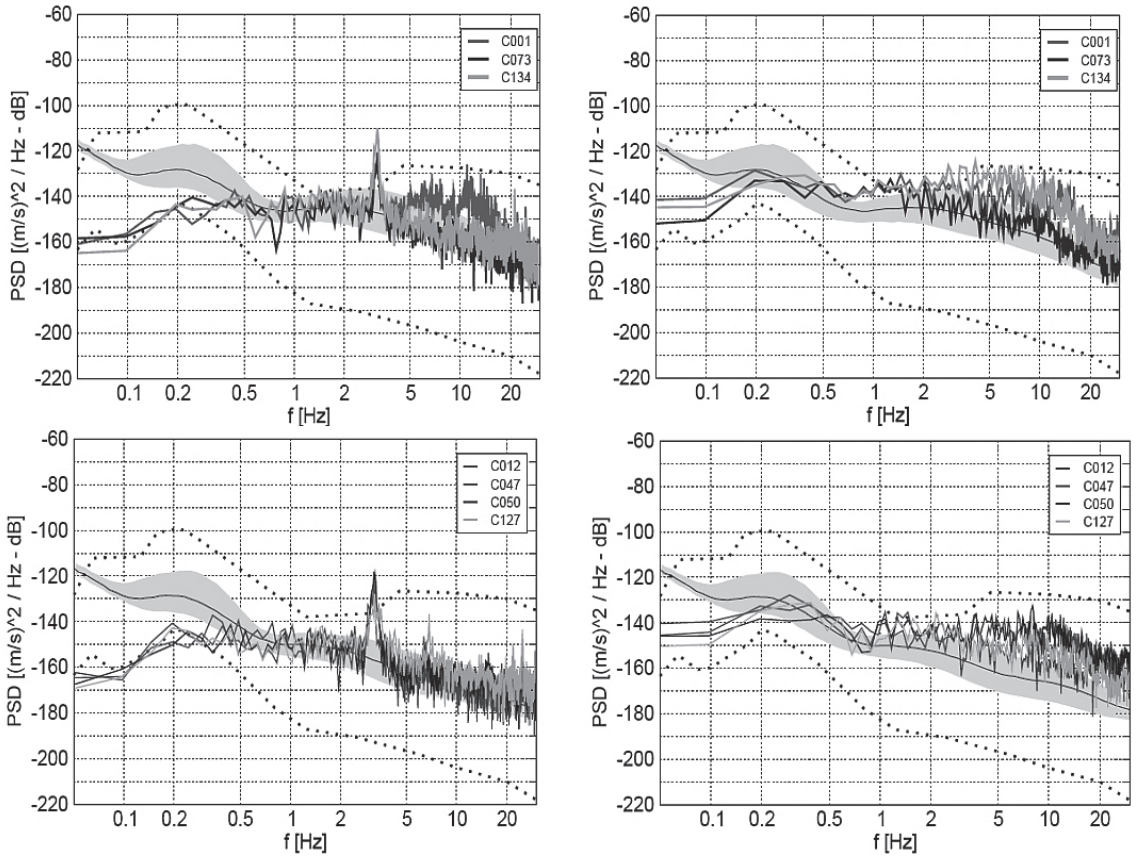

Fig. 10 - Left panels: horizontal component velocity power spectra of D-type events recorded on February 26, 2012. Right panels: horizontal component velocity power spectra of E-type events recorded on February 3, 2012. Upper and lower panels show the power spectra recorded with surface and borehole stations, respectively. Recorded power spectra are compared with the seismic ambient noise measurements (gray areas) and with the reference noise levels of Peterson (1993) (dotted lines).

power spectral density of -145 dB, with annual and monthly variability of 10 and 20 dB, respectively. Borehole (100-m depth) installations reduce the recorded average noise up to -155 dB and limit annual and monthly variability to 6 and 10 dB, respectively. In general, borehole installations at shallow depths improve the quality of the recorded signal even though they do not necessarily ensure a significant ambient noise reduction. Seismic noise levels recorded by borehole instruments depend on many factors, such as the installation depth, the subsurface geology of the recording site, and the type of ambient noise produced by human activities that characterize the installation area. A study of the borehole installations of the Italian National Seismic Network reveals that the mean level of ambient noise recorded by sensors installed at depths ranging between 50 and 175 m can undergo variations of up to 40 dB in the frequency band 1-20 Hz (see Marzorati *et al.*, 2011: Fig. 6). Stations located in the soft sedimentary layers of the central part of the Po Plain, at more than 150-m depth, show average levels of noise that are comparable with the HNM curve of Peterson (1993). Much higher noise level reductions are observed by considering shallower borehole installations in more competent rock formations (see Spriggs *et al.*, 2014). Nevertheless, the use of borehole stations increases the average

detection threshold of the network by reducing the detectable local magnitude by at least 0.3 units of magnitude. In average conditions of noise, for events occurring at 1 km hypocentral distance, the minimum observable value of local magnitude decreases from 0.1 to -0.2 when borehole stations are employed. Moreover, for earthquakes located at the same distance and using, as reference, the maximum level of noise recorded at surface and at depth during this 2-year period, the minimum observable M_L decreases from 0.8 to 0.3. We obtained this result by employing the 95 percentile PDF curves obtained at stations C073 and C050, respectively (see Figs. 5C and 5D). Therefore, even in the presence of high levels of microtremors, the installation of borehole stations maintains an adequate detection threshold for seismic events that may occur at the depth of the reservoir.

Acknowledgments. We would like to thank D. Stoll, E. D'Alema, and S. Marzorati for their willingness to make available their expertise during the installation phase of the network and the STOGIT staff at the operative centres of Cortemaggiore (PC) and of Crema (CR) for supporting the necessary maintenance operations. In particular we thank E. Marchesi, A. Cremonesi, M. Liberati, and D. Marzorati. We also thank the reviewer, E. Priolo, and the editor, M. Mucciarelli, for the careful reading of our manuscript and the valuable comments. This research has benefited from funding provided by "Stogit S.p.A. - Eni" in the framework of the "Trial Project for the injection and sequestration of CO_2 in the storage reservoir of Cortemaggiore - CO_2 Cortemaggiore Project". A preliminary version of this paper was the object of an oral presentation at the workshop "Geoitalia 2013 - IX Forum Italiano di Scienze della Terra (Pisa, Italy, September 2013)".

REFERENCES

Anderson J.G. and Hough S.; 1984: *A model for the shape of Fourier amplitude spectrum of acceleration at high frequencies*. Bull. Seismol. Soc. Am., **74**, 1969-1994.

Augliera P., D'Alema E., Franceschina G., Marzorati S., Massa M., Pessina V. and Piccarreda D.; 2010: *Installazione ed avvio rete microsismica - Sito di Cortemaggiore*. Progetto STOGIT - Realizzazione di un monitoraggio della microsismicità naturale e/o indotta nell'area pool A del giacimento di Cortemaggiore nell'ambito del progetto pilota di campo, Rendiconto, 24 pp. (in Italian).

Augliera P., Franceschina G., Massa M., Lovati S., D'Alema E. and Marzorati S.; 2011a: *Livelli di detezione da stazioni sismiche in pozzo*. In: Riassunti estesi, I° Workshop Tecnico, Monitoraggio sismico del territorio nazionale: stato dell'arte e sviluppo delle reti di monitoraggio sismico, pp. 68-71, (in Italian).

Augliera P., Franceschina G., Massa M., Lovati S., Zupo M., Marzorati S. and D'Alema E.; 2011b: *Monitoraggio della microsismicità naturale e/o indotta nel periodo febbraio 2010 - aprile 2011 - Sito di Cortemaggiore*. Progetto STOGIT - Realizzazione di un monitoraggio della microsismicità naturale e/o indotta nell'area pool A del giacimento di Cortemaggiore nell'ambito del progetto pilota di campo, Rendiconto, 43 pp. (in Italian).

Augliera P., Franceschina G., Massa M., Lovati S., Marzorati S. and D'Alema E.; 2012: *Monitoraggio della microsismicità naturale e/o indotta nel periodo maggio 2011 - aprile 2012 - Sito di Cortemaggiore*. Progetto STOGIT - Realizzazione di un monitoraggio della microsismicità naturale e/o indotta nell'area pool A del giacimento di Cortemaggiore nell'ambito del progetto pilota di campo, Rendiconto, 39 pp. (in Italian).

Bigi G., Bonardi G., Catalano R., Cosentino D., Lentini F., Parotto M., Sartori R., Scandone P. and Turco E. (eds); 1992: *Structural model of Italy 1:500,000, Sheet 1*. CNR Progetto Finalizzato Geodinamica, SELCA, Firenze, Italy.

Boiardi B.; 2012: *Pianificazione del monitoraggio di un sito in terraferma: l'esperienza italiana a Cortemaggiore e Besenzone*. In: Eni e&p, Seminario "Il monitoraggio della CCS", Osservatorio CCS, Roma, Italy, 19 pp. (in Italian).

Brune J.N.; 1970: *Tectonic stress and the spectra of seismic shear waves from earthquakes*. J. Geophys. Res., **75**, 4997-5009.

Carminati E., Lustrino M., Cuffaro M. and Doglioni C.; 2010: *Tectonics, magmatism and geodynamics of Italy: what we know and what we imagine*. In: Beltrando M., Peccerillo A., Mattei M., Condicelli S. and Doglioni C. (eds), The Geology of Italy: tectonics and life along plate margins, J. Virtual Explorer, Electronic Edition, **36**, 1-64.

Castro R., Pacor F., Puglia R., Ameri G., Letort J., Massa M. and Luzi L.; 2013: *The 2012 May 20 and 29, Emilia earthquakes: S-wave attenuation, acceleration source functions and site effects*. Geophys. J. Int., **195**, 597-611, doi:10.1093/gji/ggt245.

EU Geocapacity; 2009a: *Assessing european capacity for geological storage of carbon dioxide, D42 - GeoCapacity final report*. EU-FP6 Project no. SES6-518318, Geological Survey of Denmark and Greenland (GEUS), 63 pp., http://www.geocapacity.eu.

EU Geocapacity; 2009b: *Assessing european capacity for geological storage of carbon dioxide, D16 - WP2 Report: storage capacity.* EU-FP6 Project no. SES6-518318, Geological Survey of Denmark and Greenland (GEUS), 166 pp., http://www.geocapacity.eu.

Fantoni R. and Franciosi R.; 2010: *Tectono-sedimentary setting of the Po Plain and Adriatic foreland*. Rend. Fis. Acc. Lincei, **21**, S197-S209.

Galadini F., Poli M.E. and Zanferrari A.; 2005: *Seismogenic sources potentially responsible for earthquakes with M ≥ 6 in the eastern Southern Alps (Thiene - Udine sector, NE Italy)*. Geophys. J. Int., **161**, 739-762.

Global CCS Institute; 2013: *The Global Status of CCS: 2013*. Global CCS Institute, Melbourne, Australia, 201 pp.

Hanks T.C. and Kanamori H.; 1979: *A moment magnitude scale*. J. Geophys. Res., **84**, 2348-2350.

Hanks T.C. and Boore D.M.; 1984: *Moment-magnitude relations in theory and practice*. J. Geophys. Res., **89,** 6229-6235.

IEA; 2009: *Technology roadmap: carbon capture and storage*. OECD/IEA, Paris, France, 52 pp.

IEA; 2013a: *Redrawing the energy-climate map*. OECD/IEA, Paris, France, 134 pp.

IEA; 2013b: *Technology roadmap: carbon capture and storage*. OECD/IEA, Paris, France, 60 pp.

Konno K. and Omachi T.; 1998: *Ground-motion characteristics estimated from spectral ratio between horizontal and vertical components of microtremor*. Bull. Seismol. Soc. Am., **88**, 228-241.

Lay T. and Wallace T.C.; 1995: *Modern global seismology*. Academic Press, San Diego, CA, USA, 221 pp.

Marzorati S., Cattaneo M., D'Alema E., Frapiccini M., Ladina C. and Monachesi G.; 2011: *Sensori in pozzo della RSN dell'INGV.* In: Riassunti estesi, I° Workshop Tecnico Monitoraggio sismico del territorio nazionale: stato dell'arte e sviluppo delle reti di monitoraggio sismico, pp. 72-75 (in Italian).

McNamara D.E. and Buland R.P.; 2004: *Ambient noise levels in the continental United States*. Bull. Seismol. Soc. Am., **94**, 1517-1527.

Metz B., Davidson O., de Coninck H., Loos M. and Meyer L. (eds); 2005 IPCC special report on: *Carbon dioxide capture and storage*. Cambridge University Press, Cambridge, UK, 431 pp.

Molinari I., Argnani A., Morelli A. and Basini P.; 2015: *Development and testing of a 3D seismic velocity model of the Po Plain sedimentary basin, Italy.* Bull. Seismol. Soc. Am., **105**, 753-764, doi:10.1785/0120140204.

Nicol A., Carne R., Gerstenberger M. and Christophersen A.; 2011: *Induced seismicity and its implications for CO_2 storage risk*. Energy Procedia, **4**, 3699-3706.

Peterson J.; 1993: *Observation and modelling of seismic background noise*. USGS, Open file Report 93-322, 95 pp.

Spriggs N., Bainbridge G. and Greig W.; 2014: *Comparison study between Vault seismometers and new Posthole seismometers*. In: EGU General Assembly, EGU2014-6441, Wien, Austria, poster paper, <http://www.nanometrics.ca/microseismic/technical-resources>.

Stabile T.A., Iannaccone G., Zollo A., Lomax A., Ferulano F., Vetri M.L.V. and Barzaghi L.P.; 2013: *A comprehensive approach for evaluating network performance in surface and borehole seismic monitoring*. Geophys. J. Int., **192**, 793-806, doi:10.1093/gji/ggs049.

Tapley W.C. and Tull J.E.; 1992: *SAC - Seismic Analysis Code, USERS MANUAL, Rev. 4*. University of California, Berkeley, CA, USA, 440 pp.

Tramelli A., Troise C., De Natale G. and Orazi M; 2013: *A new method for optimization and testing of microseismic networks: an application to Campi Flegrei (southern Italy)*. Bull. Seismol. Soc. Am., **103**, 1679-1691, doi:10.1785/0120120211.

Ugalde A., Villaseñor A., Gaite B., Casquero S., Martí D., Calahorrano A., Marzán I., Carbonell R. and Estaun A.P.; 2013: *Passive seismic monitoring of an experimental CO_2 geological storage site in Hontomín (northern Spain)*. Seismol. Res. Lett., **84**, 75-84, doi:10.1785/0220110137.

Verdon J.P., Kendall J.M., White D.J., Angus D.A., Fisher Q.J. and Urbancic T.; 2010: *Passive seismic monitoring of carbon dioxide storage at Weyburn*. The Leading Edge, **29**, 200-206.

Zoback M.D. and Gorelick S.M.; 2012: *Earthquake triggering and large-scale geologic storage of carbon dioxide*. Proc. Natl. Acad. Sci. USA, **109**, 10164-10168, doi:10.1073/pnas.1202473109.

Corresponding author: Gianlorenzo Franceschina
Istituto Nazionale di Geofisica e Vulcanologia, sezione di Milano
via A. Corti 12, 20133 Milano, Italy
Phone: +39 02 23699452; fax: +39 02 23699458; email:gianlorenzo.franceschina@ingv.it